[Commentary]

Historical Perspective on Pump Fluids Engineering Technology -Response to Receiving the "Fluid Machinery Design Award" from the ASME Fluids Engineering Division-

Akira GOTO*

Abstract

To mark receiving the "Fluid Machinery Design Award" from the ASME Fluids Engineering Division, advances in experimental, numerical, and design technologies for fluid machinery over the last 40 years are reviewed based on the author's experience. Advances include pressure probe measurements downstream from a rotating impeller, multi-color oil-film flow visualization of complex secondary flows, various levels of CFD technology, 3D inverse design method for logically controlling internal flows, multi-objective optimizations for controlling performance curves, and adjoint method for optimizing complex 3D configurations. Future prospects are also discussed.

Keywords: Tow-hole Pitot probe, Multi-color oil-film flow visualization, Computational Fluid Dynamics, Inverse design method, Numerical optimization, Multi-objective optimization, Adjoint method

1. Preface

On July 12, 2016, I had the honor of receiving the "Fluid Machinery Design Award" (**Figure 1**) from the Fluids Engineering Division of the American Society of Mechanical Engineers (ASME). This biennial award was established in 1980 to honor excellence in the design of machinery involving significant fluid mechanics principles, which benefit mankind, as exemplified by application in products within the past decade. This year is the 90th anniversary of the formation of the Fluids Engineering Division. I also had the honor of receiving the 90th Anniversary Award Medal (**Figure 2**) as one of the contributors to the ASME Fluids Engineering Division over the last 90 years. I am the only Japanese among 91 recipients, which is really a great honor.

The ASME Fluids Engineering Division was established in 1926, which was just before the patent filing for a gas turbine engine by Sir Frank Whittle.

Fig. 1 Fluid Machinery Design Award

Fig. 2 90th Anniversary Award Medal

* Fluid Machinery & Systems Company

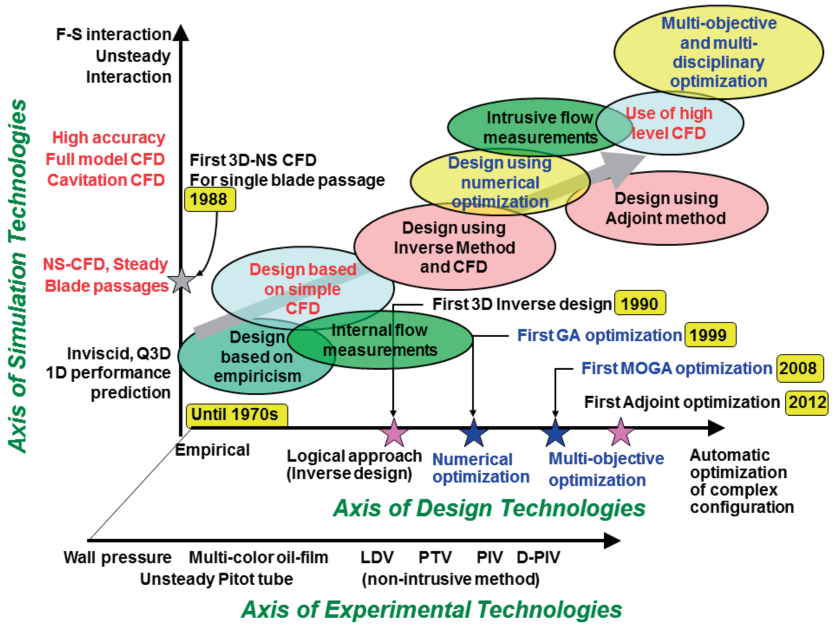

Fig. 3 Advances in experimental, numerical and design technologies

Since then, there have been enormous technological advances in fluids engineering. I have been working on experimental and numerical research, as well as design technology developments, for fluid machinery, while receiving the benefits of significant advances in computer science. To mark receiving the award, this article reviews technological advances during the past four decades.

Figure 3 presents technological advances in the fields of experimental and numerical research, as well as design technologies for fluid machinery. Each axis of technological evolution is based on achievements at Ebara Corporation, which may not be consistent with global trends. Nevertheless, advances in each technology are reviewed and forecasts are made referring to the accomplishments of the author.

2. Advances in Experimental Technology

2.1 Two-hole Pitot tube

In the early 1980s, a pump performance prediction method was developed by combining a quasi-3D flow analysis for inviscid fluids and 1D loss models. To clarify the loss-generation mechanism in impellers, a 2-hole Pitot tube with a high-frequency response was developed for measuring impeller exit flows[1]. **Figure 4** presents the construction of the 2-hole Pitot tube. Two diffusion-type semiconductor pressure sensors were placed in the stem tube with a diameter of 6 mm. Each sensor was connected to the pressure hole on the probe head using a pressure line filled with silicone oil with viscosity adjusted, which achieved a pressure-sensing system with a high resonance frequency of about 5.6 kHz. Compared to the 5-hole Pitot probe, proposed at that time, with 5 pressure transducers in the stem tube, the 2-hole Pitot probe has an extremely compact probe head and small stem tube diameter, which contributes to reducing its influence on flow fields.

The invention of the 2-hole Pitot tube was motivated by periodic multi-sampling of a slanted single hot wire to measure 3D flows behind an impeller proposed by the research group of Prof. Masahiro Inoue at Kyushu University[2]. At first, attempts were made to use a single-hole Pitot tube for measuring 3D flows. However,

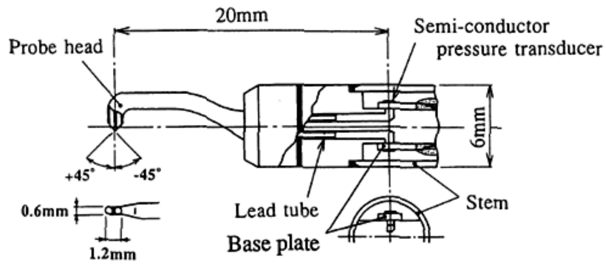

Fig. 4 Two-hole Pitot probe with high frequency response

the sensitivity of the pressure hole was poor against the flow angle change, so the concept of a 2-hole Pitot probe was adopted to guarantee measurement accuracy. The personal computer used for the measurements employed an 8-bit CPU with a 64 kB main memory and a floppy disk unit as an external storage medium. As a result, a special program was written using machine language to speed up the entire process of data sampling, processing, and storage.

Exit flow measurements and Computational Fluid Dynamics (CFD) computations were performed for a mixed-flow pump impeller with a specific speed of 560 (m^3/min, m, min^{-1})[3], see **Figure 5**. **Figure 6** (a) shows the secondary flow pattern on a quasi-orthogonal plane inside the impeller predicted with CFD computations, which suggests the accumulation of high loss fluids in the interaction region between tip leakage flows and blade-to-blade secondary flows. Impeller exit flow measurements across the stall point show the movement of the high loss region towards the blade suction surface-shroud corner at reduced flow rates (Fig. 6 (b)), its sudden expansion (Fig. 6 (c)), and the resulting sudden reduction in the pump head (stall phenomena or onset of positively sloped flow-head characteristics)[4]. Note here that clarifying complex secondary flow phenomena led to the invention of new devices for actively controlling stall and surge phenomena in pumping systems, which employ jet injection at the impeller inlet along the casing[5].

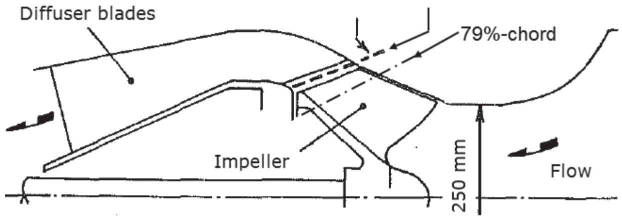

Fig. 5 Exit flow measurements by two-hole Pitot tube

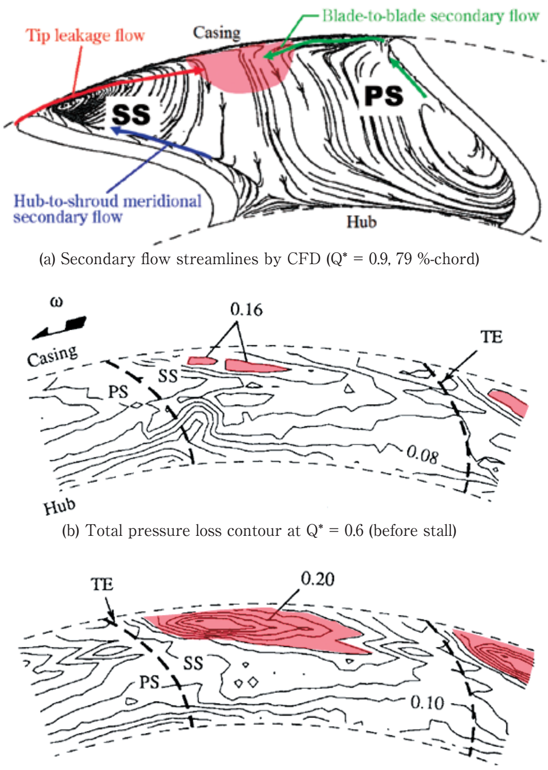

(a) Secondary flow streamlines by CFD (Q* = 0.9, 79 %-chord)

(b) Total pressure loss contour at Q* = 0.6 (before stall)

(c) Total pressure loss contour at Q* = 0.54 (just after stall)

Fig. 6 Exit flow fields of mixed-flow pump impeller

2.2 Multi-color oil-film method

During a two-year stay from 1988 at the Whittle Laboratory, University of Cambridge, I was working on an experimental investigation into an axial flow compressor stage, when I came across an oil-film flow visualization technique using a red fluorescent powder. Following this experience, after returning to Japan in 1990, we developed a multi-color oil-film flow visualization technique using red, blue, yellow, and green fluorescent powders[6].

Conventional oil-film methods sometimes use red, white, and yellow pigments. However, their specific gravities are from 4 to 9, which affect the wall surface streamlines on rotating components due to the large gravity difference between oil-film and water. It is also difficult to obtain fine streamlines, especially with intermediate colors. Moreover, the compound process of pigments, oil, additives, and dispersant depends heavily on experience, and reproducibility is not sufficient. On the other hand, the oil-film technique proposed here has the characteristic features of: 1) clear streamlines with fluorescent powder; 2) uniform and small particles (5 μm) generating fine streamlines with intermediate colors; 3) specific gravity of the powder is around 1.3 irrespective to its color, generating an oil-film having a similar specific gravity to water; and, 4) behavior of oil-film is very stable and is less dependent on experience.

Figure 7 presents the oil-film pattern obtained for a

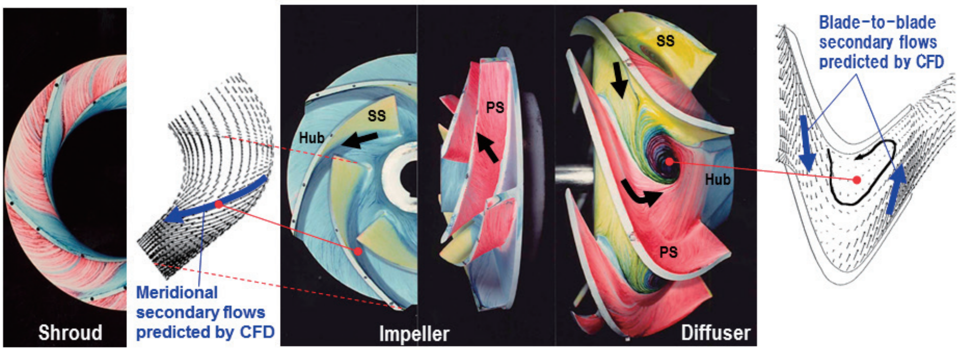

Fig. 7 Multi-color oil-film flow visualization for mixed-flow pump at design point

mixed-flow pump stage with a specific speed of 280 (m^3/min, m, min^{-1}). The hub and shroud surfaces are painted with a blue oil-film, blade suction surface with a yellow oil-film, and blade pressure surface with a red oil-film. Then, the pump is operated for around 5 minutes. The resulting wall surface streamlines present meridional secondary flows (blue colors) from the hub to the shroud on the blade suction surface (SS), blade-to-blade secondary flows (red colors) on the shroud surface originating in the meridional secondary flows on the blade pressure surface (PS), secondary flows (yellow colors) in the fore part of the diffuser channel from the suction surface (SS) to the hub surface, secondary flows (red colors) in the aft part of the diffuser channel from the pressure surface (PS) to the hub surface, and a massive separation vortex (intermediate colors) originating from the interaction zone of the secondary flows on the diffuser hub surface.

Figure 8 is a sketch of typical flow patterns on the inner surface of the impeller shroud, see the leftmost photo in Fig. 7. The flow pattern is dominated by blade-to-blade secondary flows (Type A) at over 80% flow of the design point. When the flow rate is reduced further, a small separation vortex is initiated at the corner between the blade suction surface and the shroud (Type B). This vortex develops as the flow rate is reduced (Type C), and finally spins out from the blade passage to the upstream initiating inlet recirculation (Type D), and fully developed inlet recirculation (Type E). In the present impeller, a Type B flow pattern appears at around a 70% flow, and a mixture of Types B, D, and E appears depending on the blade passages between a 68 and 66% flow, and finally all flow passages are occupied with a Type E flow pattern below a 65% flow rate[7]. So, the multi-color oil-film technique is effective for visualizing secondary flow behaviors and clarifying abnormal flow phenomena at partial operating conditions. The flow patterns obtained have been useful for CFD code validation.

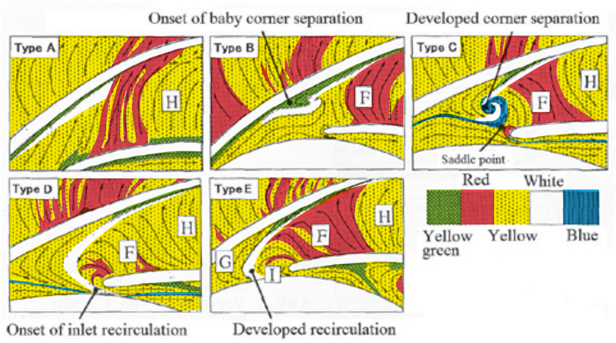

Fig. 8 Typical flow pattern on shroud surface at partial flows rates

2.3 Non-intrusive flow fields measurements

A non-intrusive method of flow measurements (without disturbing flow fields by probe insertion) such as laser Doppler velocimetry (LDV) has been applied to pump internal flows since the 1980s. More recently, particle image velocimetry (PIV) has been applied to measure instantaneous flow fields in fluid machinery, and measurements of the turbulent boundary layer structure close to wall surfaces have been challenged recently.

Many of the technical problems we face these days involve unsteady flow phenomena, so expectations for PIV are large. However, its applications to pump internal flows are still limited. A great breakthrough may be achieved by hybridizing experiments and computations and new techniques for handling cavitating flows.

3. Advances in Computational Methods

The top 500 Lists (https://www.top500.org/lists/) for supercomputers show the speed of floating-point calculations increasing 10 times every 3 to 4 years. A more important fact is that computing power, comparable to the world's No. 1 supercomputer, became available industrially after 10 years. A simplified estimation of the design space suggests that engineering computations requiring one year can be done in half a day after those 10 years, and 700 times design case evaluations can be done with engineering computations. In reality, the increase in the speed of engineering computations may not be so significant, because: 1) more detailed CFD modeling is adopted (e.g. including small gaps); 2) bigger models are adopted (e.g. full-stage analysis of a multi-stage pump instead of a single-stage analysis); 3) improvements in numerical accuracy (e.g. use of a more detailed turbulence model using extremely fine meshes); 4) use of unsteady computations (handling more realistic time-dependent flows rather than time-averaged flows); and, 5) extension of the scope of numerical computations (e.g. numerical evaluation of cavitation phenomena). Nevertheless, there is no doubt that engineering processes employing numerical computations will change dramatically, and advances in computational science have great impacts on manufacturing industries.

Figure 9 (a) shows a typical computational mesh for a mixed-flow pump stage in the 1990s[8]. To simplify mesh generation, the tip clearance is modeled by rounding up the blade tip. A virtual shaft is assumed upstream from the impeller so as not to change the mesh topology around the central axis. Computational costs are reduced by calculating a single blade channel using periodic boundary conditions in the circumferential direction. For the blade number difference between impeller and diffuser, a mixing plane model is employed between impeller and diffuser to circumferentially average the flow fields using steady flow computations with the Baldwin-Lomax zero-equation turbulence model. The total number of grid points is 260000 in this case.

After 20 years had passed, in the mid-2010s, a more detailed computational model could be handled due to

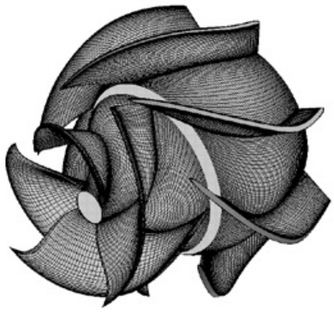

(a) Mixed-flow pump stage in 1997; 0.26 million grids/pitch

(b) Multi-stage pump in 2016; 36 million grids

Fig. 9 Change of computational model size in 20 years

big advances in computer sciences (one million times increase in the speed of floating-point calculations). Fig. 9 (b) shows a computational model used for a 5-stage high-pressure multi-stage pump[9]. Leakage flows through small gaps between sleeves and wearing rings have dominating effects at off-design operation, so those small gaps are also modeled. This pump has a variety of rotational asymmetry parts such as volute casing and long inter-stage flow channel (cross-over channel), so periodic boundary conditions cannot be used. The total number of grid points is about 36 million, modeling all internal flow passages of the multi-stage pump, and transient unsteady computations are performed by rotating the impeller with time. The k-ω SST, a two-equation turbulence model, is used here.

In addition to using refined meshes and a large computational model, the use of a turbulence model with higher accuracy has greatly advanced. For many years, Reynolds Averaged Navier-Stokes (RANS) computations, modeling all scales of turbulent eddies, have been a major tool in industries. However, a national project is progressing using a K-computer, the No. 1 supercomputer in Japan, to apply Large Eddy Simulations (LES) industrially, where only small eddies

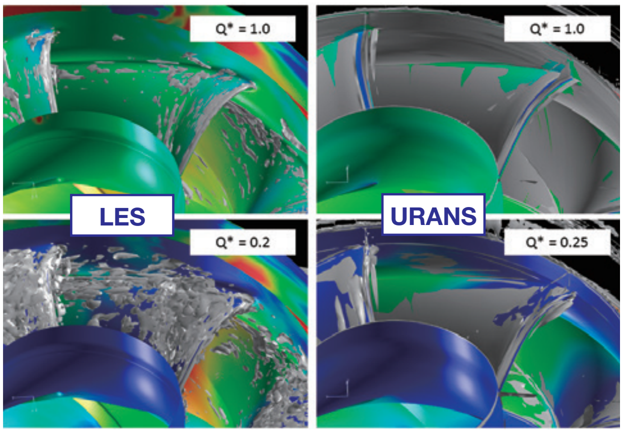

(a) LES computation (b) RANS computation

Fig. 10 Accuracy of turbulence model (Q*=1.0: design flow)

are modeled and large eddies are solved directly without modeling[10]. **Figure 10** compares the flow fields between LES computations and URANS (unsteady RANS) computations for inlet flow fields of an impeller in a double suction pump. The LES computations capture very complex vortex structures, especially under partial operating conditions, compared to URANS computations. Predicting detailed vortex structures and controlling them are key technologies for further improving performance and machine reliability, and it is expected that K-computer class supercomputing will be employed industrially in the late 2020s.

4. Advances in Design Technology

4.1 Inverse design method

Advances in computational technologies are significant, and attempts are progressing to replace experiments with computations. Computations give extremely detailed information on internal flow fields compared to experiments, which may trigger breakthroughs in issues that are difficult to tackle with experimental approaches. However, computational results do not tell us directly how we should change a design and the designer may be at a loss by having a massive amount of information. If we remind ourselves of the fact that a number of design issues still remain despite the 100-year history of detailed experimental research on the internal flows of fluid machinery, it may be understood that simply replacing experiments with advanced computational technologies will not be sufficient. It is extremely important to take up the challenge of achieving parallel advances in design technologies.

Design technology relied entirely on empirical design charts up until the 1970s. This approach is based on extensive experimental records and provides reasonable designs quickly within the scope of our experience. Naturally, such an approach cannot be sufficient for taking on big challenges that go beyond existing designs. In the conventional approach of solving direct problems (upper work flow in **Figure 11**), an initial design is made using design charts and then a trial-and-error approach is adopted either experimentally or numerically to improve the designs gradually.

On the contrary, the more logical approach of solving inverse problems has been proposed (lower work flow in Fig. 11), where ideal flow fields that satisfy an evaluation index are specified and the blade shape that achieves ideal flow fields is derived theoretically. The first inverse design method was proposed by Sir Michael James Lighthill in 1945 for the design of a 2D airfoil. The theory was extended to a 2D cascade design, and finally to a full 3D cascade design around 1990[11]. These theories are based on the inviscid flow assumption, so it is not certain if an inverse design blade profile would perform as expected in an actual viscous flow environment, which is the biggest issue for the industrial application of the method. However, due to advances in RANS CFD during the 1990s in industries, the inverse design blade can be evaluated more accurately nowadays. This has made the inverse design method a practical tool for designing a blade shape. In the mid-1990s, the 3D inverse design technology succeeded in logically controlling and optimizing secondary flows in fluid machinery for the first time[12]. The massive separation vortex in diffusers shown in Fig. 7, for example, was completely eliminated by

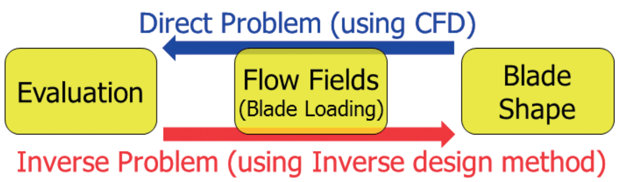

Fig. 11 Direct and Inverse Problems

controlling secondary flows in the diffuser channel[13]. The number of fluid machines (such as pumps and compressors) designed with the inverse design method and shipped from Ebara Corporation is about 29000 units as far as we know.

Figure 12 shows performance improvements for a mixed-flow pump with a specific speed of 800 (m^3/min, m, min^{-1}) over the 30 years between the 1970s and the 2000s. The 1970s design is called the base-line design, and each characteristic curve is normalized with the efficiency and the pump head for the base-line pump in the design flow. The 1990s design, employing RANS CFD computations, succeeded in improving peak efficiency by 8.7 points and eliminating instability in the flow-head curve (stall phenomena) at around a 60% flow. Note here that the maximum pump diameter is larger than the base-line design by as much as 24%. On the other hand, the 2000s design, employing a 3D inverse design method, succeeded in improving peak efficiency by 11.6 points from the base-line by controlling secondary flows in the impeller and the diffuser. The maximum diameter is much smaller than the 1990s' design and is larger than the base-line by 9%.

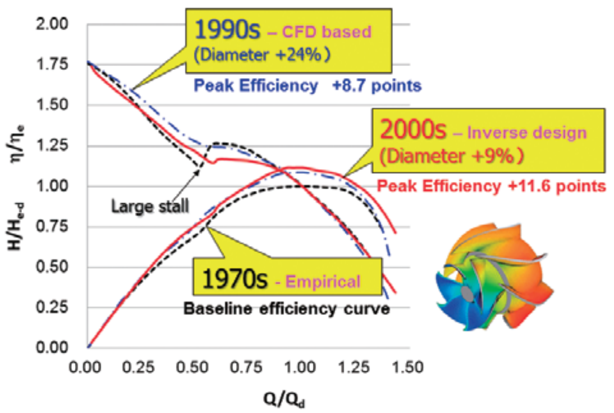

Fig. 12 Performance improvements over past 30 years

Figure 13 presents an inverse design of mixed-flow pump stages having a specific speed of 800 (m^3/min, m, min^{-1}), which satisfies the same design specification. If we adopt an empirical approach, the optimal meridional configuration is determined based on the design specific speed. However, the inverse design approach is adopted here, targeting two different objectives of high efficiency and super compact machine size. Fig. 13 (a) achieves a peak efficiency improvement of 5.8 points compared to the best conventional design having a similar machine size. On the other hand, Fig. 13 (b) achieves a super compact machine size of 40% of the conventional design with a similar peak efficiency level[8]. If we adopt the super compact design for water jet propulsion, for example, its compact size contributes to securing ship space, and significant improvements in propulsion efficiency for the ship itself are achieved due to the light weight of the pump. It is clearly understood that the logical approach employing the inverse design method could offer great value to each customer beyond the limits of the conventional empirical approach.

4.2 Numerical optimization

Because of remarkable advances in computational power during the 2000s, numerical optimization has become very actively applied. **Figure 14** introduces 2 typical numerical optimization algorithms that reference mountain climbing. The Gradient Method (GM) changes the design variables in the direction that gives the biggest improvements to objective functions (e.g.

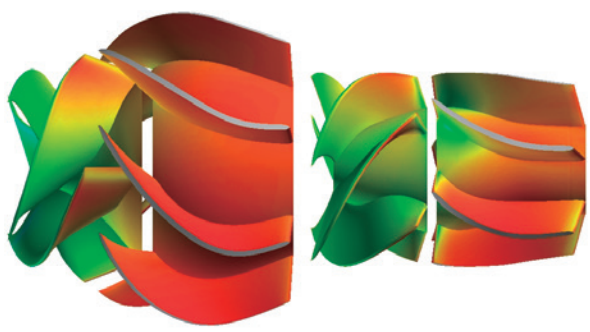

(a) High efficiency design (b) Super compact design

Fig. 13 Inverse design of mixed-flow pump stage

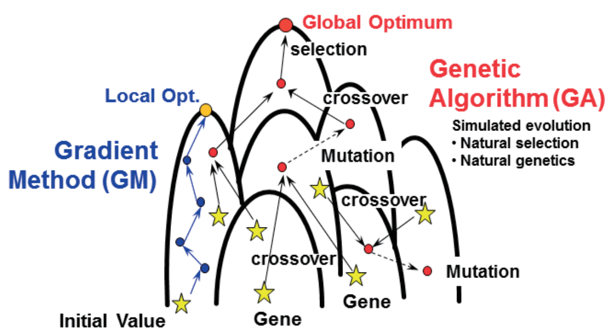

Fig. 14 Algorithm of numerical optimization

efficiency); i.e., the biggest gradient between objective function and design variables. GM is a very efficient optimization algorithm requiring relatively small computational power and always reaches the optimal value (top of the mountain). However, it is well-known that the optimization problem involving fluids phenomena is almost always a multi-peak problem due to the strong non-linearity of the governing equations. So, depending on the initial design values (where we start climbing the mountain), the optimal solution differs and almost always ends up with a local optimum, and it is difficult to reach a global optimum.

To overcome the disadvantages of GM, an exploratory numerical optimization approach such as the Genetic Algorithm (GM) was proposed. GA describes different combinations of design variables using a gene sequence, and simulates the nature of the evolutional process by adopting good genes and crossing them, which gives good objective function values. By exchanging the dominant gene and introducing a mutation, GA reaches the global optimum even for multi-peak optimization problems. The disadvantage of GA is the fact that it requires a large number of individuals (design cases) evolving over many generations, which requires large computational resources. This is especially true for cases with many design variables (i.e. long gene sequence), which often make it practically impossible to perform numerical optimization.

Before the establishment of the inverse design approach in 1990, all of the design theories were based on a direct design approach, which tries to link blade configuration parameters (design variables) to machine performance (objective functions). The flow passages of high-performance fluid machinery are mostly composed of complex 3D free surfaces, which require a large number of design variables to define the surfaces, and the design space tends to become very large. Imagine changing each design variable for three levels (large, intermediate, and small) and estimating the number of design cases with all combinations of design variables. Eight design variables give 6561 cases ($=3^8$); 18 design variables give 390 million cases; and, 30 design variables give 206 trillion cases. If we assume a few hours of CFD computations for each case, it is easy to understand that the hours required to explore the design space would be impractical with an increase in the number of design variables.

To define the 3D free surface of an impeller blade with the direct design approach, 20 design variables are possibly required to maintain a sufficient level of freedom. This would require large computational resources. On the contrary, the inverse design approach has a number of advantages: 1) complex 3D free surfaces can be generated very quickly (within one minute) using a small number of design variables (typically 8 parameters); 2) the design case always satisfies the design specification; and, 3) the correlation between design variables (blade loading distributions) and objective functions (performance) is very smooth. Based on these features, a numerical optimization hybridizing GA with the inverse design approach was proposed in the early 2000s for a single objective optimization[14].

4.3 Multi-objective optimization

In the real world, almost all optimization problems are multi-objective problems. **Figure 15** shows the wide range of performance characteristics predicted with CFD for various combinations of design variables for a mixed-flow pump with a specific speed of 1300 (m^3/min, m, min^{-1}). In addition to high efficiency and sufficiently high suction performance, markets often request a lower shut-off head (maximum head) to reduce the

Fig. 15 Performance characteristics of mixed-flow pump

flange rating of the plant piping, lower shut-off power (maximum power) to decrease the motor rating for reduced cost, and a stable flow-head characteristic curve to avoid system instability (suppress stall phenomena) in pump-piping systems. However, there are trade-off relationships among these performance characteristics and it is impossible to maximize (or minimize) the requirements at the same time.

Fig. 15 suggests that we can design pumps with various performance characteristics (such as peak efficiency, shut-off head, shut-off power, and stall characteristics) by adopting suitable design variables, while keeping the design specification the same. Based on this understanding, a multi-objective optimization of mixed-flow pump performance characteristics was proposed in 2009[15]. In the design space of multi-objective optimization created by various combinations of design variables, a set of solutions called Pareto solutions is derived, where further improvements to one objective function inevitably lead to a deterioration of one of the other objective functions. Pareto solutions compose solution boundaries that cannot be crossed with any combination of optimized design variables. One example of a Pareto front is presented in **Figure 16** for three objective functions. The optimization problem results in a trade-off selection in the design on the Pareto front surface.

When the number of objective functions is less than three, the Pareto front obtained can be visualized as solution surfaces on a 2D plane or on a 3D space. However, if the number of objective functions is four or more, it is not easy to visualize the solution space of the Pareto front. One of the visualization techniques for

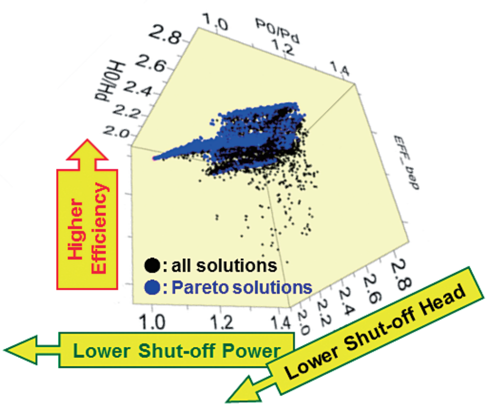

Fig. 16 Pareto solutions (trade-off solutions)

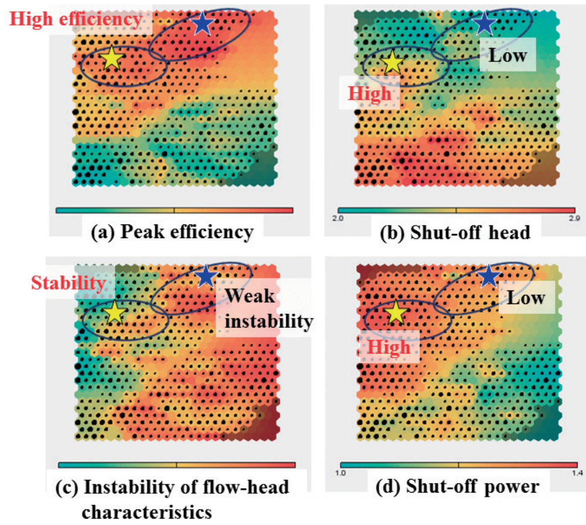

Fig. 17 Self-organizing map for Pareto solutions
(★ : Design case #1, ☆ : Design case #2)

the characteristic feature of the Pareto solution space is to use a Self-Organizing Map (SOM) as the data-mining method. **Figure 17** shows the SOM for the optimization problem in Fig. 15. The corresponding dot on each SOM represents a specific design case on the Pareto front and the value of each objective function is shown as color contours on each SOM. For example, design case #1 represents the Pareto solution that gives a low shut-off head, acceptable instability, relatively low shut-off power, and sufficiently high efficiency. Design case #2, prioritizing stability characteristics, represents the Pareto solution with high shut-off head, high stability, and reasonably good peak efficiency. If we prepare such SOMs in advance, a design meeting the requirements of a specific customer can be selected quickly.

Almost all optimization problems have multi-objective and multi-disciplinary natures. It will become more and more important to perform multi-objective and multi-disciplinary optimization involving other technical fields in addition to fluids engineering technology. For example, morphology design of a multi-stage vertical shaft pump has been challenged for a multi-disciplinary optimization prioritizing rotor-dynamics stability over fluid-dynamic performances[16]. Besides, a visualization technique for the solution space, such as that in Fig. 17, is important to allow quick trade-off selections in a multi-objective optimization.

4.4 Optimization of complex flow passages

In the previous sections, the 3D inverse design method and its combination with numerical optimization are presented as an effective design tool for blade profiles. In addition to blade components, there are various stationary flow passages with complex 3D configurations in fluid machinery, which also have an important impact on machine performance and reliability. **Figure 19** (a) shows one example of a 2-stage high-pressure pump having a suction chamber upstream from the impeller, diffuser channels downstream from the impeller, inter-stage flow channel, and volute casing at the outlet from the second stage. All of these stationary flow passages have very complex configurations composed of complex 3D free surfaces and it is troublesome to model these configurations using 3D-Computer Aided Design (CAD). To maintain the freedom of 3D surfaces, it is necessary to use many design variables in CAD modeling. In this case, the computational costs are unacceptably high if an exploratory type of optimization such as GA is adopted for optimizing a parameterized CAD model.

To solve the issue mentioned above, a new optimization method has been proposed based on an adjoint approach[17]. The adjoint method is extremely effective for optimizing a complex configuration, because all of the mesh points of the model are adopted as design variables, while keeping computational costs at the same level as regular CFD computations. The mesh points are gradually shifted in a direction to minimize (or maximize) the specified objective function using the Gradient Method (GM); see **Figure 18**. This method is based on GM and is not truly suitable for multi-peak optimization problems. So, it is important to design a reasonably good initial configuration of the flow passage using a conventional design, for example. The sensitivity vectors obtained in the adjoint optimization process are a good guideline, suggesting suitable areas for modification and their deforming directions, even for manual optimization using a parameterized 3D-CAD model.

Fig. 19 shows the results of adjoint optimization for diffuser and inter-stage flow passages using one objective function, which conforms to the two objectives of minimizing total pressure losses and maximizing flow uniformity at the outlet of the flow passage under 50/50 percentage weight[18]. In conventional design practice, the diffuser channels are in rotational symmetry. Adjoint optimization, however, gives different diffuser channel sensitivities (area of deformation and its amount) depending on the circumferential position of the diffuser channel because of the interaction with downstream inter-stage flow passages; see Fig. 19 (b). The final optimized configuration in Fig. 19 (c) shows very a complicated configuration, which is difficult to achieve with a 3D-CAD-based trial-and-error approach, and the

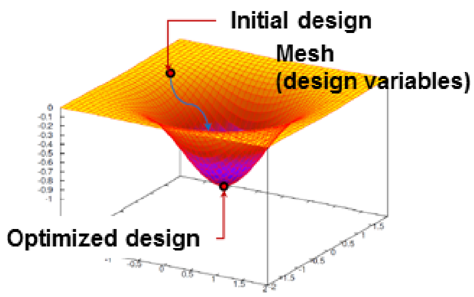

Fig. 18 Adjoint optimization

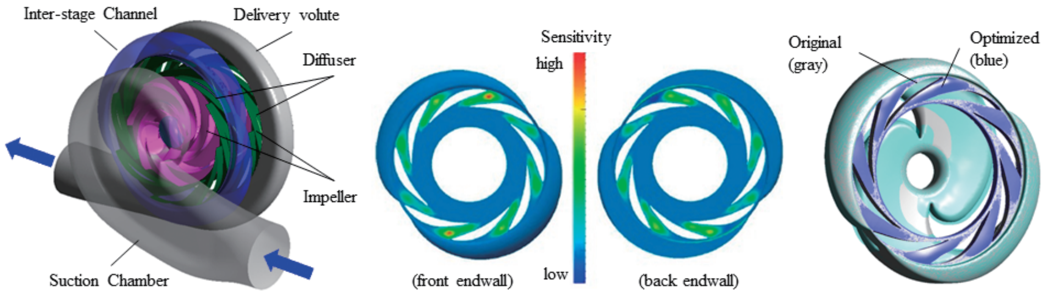

(a) High-pressure pump (b) Sensitivity analysis of diffuser endwalls (c) Optimized diffuser channel

Fig. 19 Adjoint optimization of high-pressure 2-stage multi-stage pump effectiveness of the adjoint approach can be clearly confirmed.

5. Concluding Remarks

To summarize, I would like to express my deep appreciation to my colleagues who worked on the technological developments and applications presented in this article over the years. I am also grateful for the guidance and support of professors and researchers in Japan, as well as in other countries.

Looking back over the past 40 years, developments in experimental, numerical, and design technologies have been really significant. This article briefly introduces trends of technological developments referring to concrete examples together with some prospects for the future. It is hoped it will be of use especially for young researchers who take up the challenge of inventing new fluid machinery with new tools for experiments, numerical computations, and design optimizations.

References

1) Goto, A., "Phase-Locked Measurements of Three-Dimensional Periodic Flow from an Impeller using a Two-Hole Pitot Tube", The 2nd International Symposium on Fluid Control, Measurements and Visualization (FLUCOME-2), Sheffield (1988).
2) Kuroumaru, M. et al., "Measurement of Three-Dimensional Flow Field Behind an Impeller by Means of Periodic Multi-Sampling with a Slanted Hot Wire", Bulletin of JSME, Vol. 25, No.209 (1982).
3) Goto, A., "Study of Internal Flows in a Mixed-Flow Pump Impeller at Various Tip Clearances Using Three-Dimensional Viscous Flow Computations", ASME Journal of Turbomachinery, Vol. 114 (1992).
4) Goto, A., "The Effect of Tip Leakage Flow on Part-Load Performance of a Mixed-Flow Pump Impeller", ASME Journal of Turbomachinery, Vol. 114 (1992).
5) Goto, A., "Suppression of Mixed-Flow Pump Instability and Surge by the Active Alteration of Impeller Secondary Flows", ASME Journal of Turbomachinery, Vol. 116 (1994).
6) Goto, A., "Numerical and Experimental Study of 3-D Flow Fields within a Diffuser Pump Stage at Off-Design Condition", The Joint ASME-JSME Fluids Engineering Summer Conference, Hilton Head Islands, FED-Vol. 227 (1995).
7) Goto, A., "Flow Phenomena in a Low-Specific-Speed Diffuser Pump at Partial Operating Conditions (Numerical Prediction of Impeller Inlet Recirculation)", Pump Congress, Karlsruhe (1996).
8) Goto, A., Ashihara, K., Sakurai, T., and Saito, S., "Compact Design of Diffuser Pumps using Three-Dimensional Inverse Design Method", ASME FEDSM99-6847, San Francisco (1999).
9) Suzuki, T. and Takemura, T., "CFD Analysis of Performance of Five-Stage High-Pressure Volute Pump", ASME FEDSM2016-7799, Washington DC (2016).
10) Kato, C. (Theme Leader), "Next-generation Fluid-Flow Design Systems based on Direct Computation of Turbulence", Industrial Innovation, Strategic Programs for Innovative Research (SPIRE), (2010-2015).
11) Zangeneh, M., "A Compressible Three Dimensional Design Method for Radial and Mixed Flow Turbomachinery Blades", International Journal for Numerical Methods in Fluids, Vol. 13 (1991).
12) Zangeneh, M., Goto, A., and Harada, H., "On the Design Criteria for Suppression of Secondary Flows in Centrifugal and Mixed-Flow Impellers", ASME Journal of Turbomachinery, Vol.120 (1998).
13) Goto, A. and Zangeneh, M., "Hydrodynamic Design of Pump Diffuser Using Inverse Design Method and CFD", ASME Journal of Fluids Engineering, Vol. 124 (2002).
14) Ashihara, K. and Goto, A., "Turbomachinery Blade Design using 3D Inverse Design Method, CFD and Optimization Algorithm", ASME Turbo Expo (2001).
15) Takayama, Y. and Watanabe, H., "Multi-Objective Design Optimization of a Mixed-flow Pump", ASME FEDSM2009-78348, Vail (2009).
16) Kagawa, S., et al., "Study of Morphology Design in the Industrial Vertical Multistage Pump", JSME Mechanical Engineering Congress, J1030304, Fukuoka (2016).
17) TURBOdesign Shaper, Advanced Design Technology, Ltd.
18) Sekino, Y., et al., "Optimization of High Pressure Pump Flow Passages based on Adjoint and CFD", ASME FEDSM2016-7831, Washington DC (2016).